Electronic Supplementary Information (ESI):

Prediction of Novel Semi-conducting Two-Dimensional MX_2 Phosphides and Chalcogenides (M = Zn, Cd; X= P, S, Se) with 5-Membered Rings

Esmail Amaki[a], Zabiollah Mahdavifar*[a,] Gilles Frapper*[b]

[a]Department of Chemistry, Faculty of Science, Shahid Chamran University of Ahvaz, Ahvaz, Iran.
Email: z_mahdavifar@scu.ac.ir

[b]Applied Quantum Chemistry group, IC2MP UMR 7285, Université de Poitiers, CNRS, 4, Rue Michel Brunet TSA 51106-86073, Cedex 9, Poitiers, France. Email: gilles.frapper@univ-poitiers.fr

* Corresponding Authors

Zabiollah Mahdavifar − orcid.org/0000-0002-9709-0502 ; Email: z_mahdavifar@scu.ac.ir

Gilles Frapper − orcid.org/0000-0001-5177-6691; Email: gilles.frapper@univ-poitiers.fr

Contents

S.1. Computational Methods

S1-1. Evolutionary algorithm (USPEX code) and heuristic approach

USPEX (Universal Structure Predictor: Evolutionary Xtallography, versions 10.3 and 9.4.4)[1] is a global evolutionary algorithm (EA) designed for crystal structure prediction (Global optimizer). It has been under development since 2004 in the A. R. Oganov laboratory (for more information, visit http://uspex-team.org/en/uspex/overview). It has been integrated with VASP (Vienna Ab initio Simulation Package, version 5.4.4) to enable DFT crystal structure relaxation (Local optimizer). VASP optimizes the shape, volume, and atomic positions. Initially, a 2D fixed-composition EA search was carried out in USPEX to predict the structures of two-dimensional compound ZnP_2, the stationary points on the potential energy surface (PES). [2,3] To ensure that the global minimum was reached, about ~4,500 2D structures were generated over 60 generations. Given the stochastic nature of the EA, three USPEX jobs were performed. In 2D EA searches, the thickness of 2D ZnP_2 slabs is constrained to 0-5 Å and the total number of atoms in the 2D primitive unit cell is up to 12. The vacuum size is up to 15 Å. The fitness is calculated by determining the enthalpy (at T = 0 K, G = H) obtained from an *ab initio* total energy calculation (using DFT GGA PBE as implemented in VASP).

A large number (140) of randomly created structures is chosen in the first generation of the EA. In the next generations, 100 structures are generated. 80% of the best (i.e., lowest enthalpy) optimized structures are selected to participate in producing the next generation. New candidate structure is produced from parent structures using one of three operators: (i) heredity, (ii) lattice mutations, and (iii) atomic mutation, which account for 50, 10, and 20% of the structures in the new generation. The remaining 20% are randomly generated (similarly to those of the first generation).

The five low-energy 2D structures of ZnP_2 containing 5-membered rings have been selected. Therefore, Zn is substituted by Cd, and P by S/se atoms, leading to a pool of initial structures (guesses) of 2D penta- ZnPS, ZnPSe, ZnSSe, CdP_2, CdPS, CdPSe and CdSSe.

Images of the crystalline structures were produced using the VESTA software.[4]

S1.2. DFT calculations (VASP)

Structure relaxations (shape, atomic positions) were carried out using density functional theory (DFT) as implemented in the Vienna ab initio simulation package (VASP, version 5.4.4).[5,6] We adopted the Perdew−Burke−Ernzerhof (PBE) functional[7] at the generalized gradient approximation (GGA) level of theory, with PAW potentials[8] for all atoms, a plane-wave kinetic energy cutoff of 600 eV, and a uniform, Γ-centered grid with $2\pi \times 0.03$ Å^{-1} spacing for reciprocal space sampling. A 12-15 Å vacuum layer was used to avoid interactions between neighboring supercells. A Monkhorst–Pack 14×14×1 and 12×12×1 K-points mesh was sampled for geometry optimisation and electronic structure calculations, respectively.

Subsequently, the chosen low-energy structures were re-optimized with the dispersion-corrected DFT-D3 method incorporating Becke-Johnson damping.[9] The GGA-PBE functional has been proven to be accurate in describing the structural properties of materials, although it may underestimate the band gap (E_g) values of open-gap materials such as semiconductors. Therefore, we have determined E_g at the Heyd-Scuseria-Ernzerhof (HSE06) hybrid functional level of theory,[10] using the optimized GGA-PBE structure (single point energy calculation). This level of theory is thereafter denoted HSE06//PBE.

S1-3. Phonon dispersion curves calculations

The dynamic stability of the statically relaxed 2D structures was verified by the absence of imaginary phonon frequencies. First principles phonon calculations with density functional perturbation theory (DFPT) at quasi-harmonic level were done using the open-source package PHONOPY code[11,12] (see phonon dispersion curves of 2D MX_2 phases). Supercell structures with atomic displacements were created based on the primitive unit cell and considering crystal symmetry. Typically, a 3×3 supercell is needed, sometimes higher.

S1-4. Ab initio molecular dynamics (AIMD) simulations

Ab initio molecular dynamics (AIMD) simulations based on DFT at 900K, and 1200K were carried out using the VASP code to examine the thermal stability of 2D MX_2 phases. AIMD calculations with Nosé canonical ensemble[13] were performed up to 1200 K. The time step was 1 fs, and the total simulation time was up to 5 ps. In these AIMD simulations, 4×4 supercells of ground state phases were used, and the Brillouin zone integration was limited to the Γ point of the supercell, because of the high computational expense.

S1-5. The electron localization function (ELF) and Bader charge calculations

In the context of density functional theory, the electron localization function (ELF)[14] is employed to indicate the probability of finding an electron in the neighborhood of a reference electron with the same spin and different electron interactions such as covalent and metallic chemical bonds. We performed ELF calculations to determine the nature of the chemical bonding of the 2D MP_2 (M=Zn, Cd), MSSe (M=Zn, Cd) and ZnPS monolayers. The ELFs of predicted structures are shown in Figures S16. The value of ELF is in the range of $0 \leq ELF \leq 1$. In ELF plot, the red color (ELF=1) indicates covalent bonds. From these figures, it can be seen that the electrons are mostly localized around the P, S and Se atoms and less amount of electrons localized around metal atom. Further analysis of ELF data indicates that the nature of bonds in MP_2 (M=Zn, Cd), MSSe (M=Zn, Cd) and ZnPS structures are mainly covalent in nature.

To better comprehend the electronic structure of 2D MX_2 structures, Bader charge[15] calculations were carried out. The charge density difference (ΔQ) was calculated and its results are given in Table S4. In all analysed structures, transfer of charge from Zn and Cd metal atoms to non-metal atoms P, S and Se was observed. To further scrutinize the rate of charge transfer, a charge transfer comparison diagram was plotted in Figure S17. The charge transfer rate increases with greater overlap between metallic and non-metallic states. α-CdSSe and CdP_2 structures exhibit the highest and lowest metal-to-non-metal atoms atom charge transfer, respectively. These findings confirm those of ELF analysis.

S1-6. References

1 Y. Qu, C.T. Kwok, Y. Shao, X. Shi, Y. Kawazoe, H. Pan, *Int. J. Hydrog. Energy.,* 2021, **46**, 9371-9379.

2 P.V. Bushlanov, V.A. Blatov, A.R. Oganov, *Comp. Phys. Comm.,* 2019, **236**, 1-7.

3 Z. Mahdavifar and F. Shojaei, *Phys. Chem. Chem. Phys.,* 2019, **21**, 22618-22628.

4 K. Momma and F. Izumi, *J. Appl. Cryst.,* 2011, **44**, 1272−1276.

5 G. Kresse and J. Furthmuller, *Phys. Rev. B.,* 1996, **54**, 11169- 11186.

6 G. Kresse, and J. Furthmuller, *Comput. Mater. Sci.,* 1996, **6**, 15-50.

7 J. P. Perdew, K. Burke, M. Ernzerhof, *Phys. Rev. Lett*., 1996, **77**, 3865-3868.

8 P.E. Blöchl, *Phys. Rev. B*., 1994, **50**, 17953-17979.

9 T. Chen, Q. Gu, Q. Chen, X. Wang, C.J. Pickard, R.J. Needs, D. Xing, J. Sun, *Phys. Rev. B.,* 2020, **101**, 054518.

10 J. Heyd, G.E. Scuseria, M. Ernzerhof, *J. Chem. Phys.,* 2003, **118**, 8207–8215.

11 K. Parlinski, Z.Q. Li, Y. Kawazoe, *Phys Rev Lett.,* 1997, **78**, 4063-6.

12 A. Togo and I. Tanaka, *Scripta Mater*., 2015, **108**, 1-5.

13 H. Yuan, Z. Li, J. Yang, *J. Mater. Chem. C.,* 2018, **6**, 9055-9059.

14. A. D. Becke and K. E. Edgecombe, *J. Chem. Phys*., 1990, **92**, 5397–5403.

15. R. F. W. Bader, *Atoms in Molecules - A Quantum Theory*, Oxford University Press, Oxford, 1990.

S2. Optimized phosphides and chalcogenides MX_2 structures (M = Zn, Cd; X= P, S, Se): POSCAR files

POSCAR file of α-ZnP_2

```
1.0000000000000000
  3.9340153342379534   -0.8894707850013384    0.0000000000000000
 -0.8195820028981415    5.5167741202456053    0.0000000000000000
  0.0000000000000000    0.0000000000000000   12.5926886773420250
  Zn   P
  2    4
Direct
  0.5833310725296315  0.7226094047260716  0.5834018874934230
  0.0833310725296315  0.7226094047260716  0.4165981125065770
  0.4902600864751889  0.5363014623416404  0.3694675060635362
  0.9902600864751889  0.5363014623416404  0.6305324939364638
  0.3098358409951771  0.1750761329322899  0.4497170539425497
  0.8098358409951771  0.1750761329322899  0.5502829460574503
```

POSCAR file of β -ZnP_2

```
1.0000000000000000
  6.5617303847999997    0.0000000000000000    0.0000000000000000
  3.0819482802999998    5.3380910078000001    0.0000000000000000
  0.0000000000000000    0.0000000000000000   11.6349906921000006
  Zn   P
  3    6
Direct
  0.8163381713082671  0.7793223523977275  0.4156865245042809
  0.1298171390453717  0.1159020169654070  0.4817416230591647
  0.4811275904098480  0.1475991277433479  0.6304061384534876
  0.4715668689402719  0.7581611524475633  0.4095869492456288
  0.7650812352852867  0.1451773840044979  0.4938075029705900
  0.2167378546165821  0.5947064177014667  0.6381843870862767
  0.1879503652864045  0.4662338630476199  0.4634703863030012
  0.4697731353319909  0.7427846027210592  0.6028337536925505
  0.5101678037759925  0.3931549479713112  0.3642777586850272
```

POSCAR file of ZnPS

```
1.0000000000000000
  5.4263058578852590   -0.6370917331304317    0.0839180334903804
 -0.7840905794005196    4.6678669986453265    0.1573962419966687
 -0.1779067637328123   -0.3520811345382847   16.5366534948310111
   S    P    Zn
   2    2    2
Direct
  0.5148779051508541  0.5457635761582367  0.5647361584593185
  0.9312607669478936  0.1709482293625868  0.4775789904976264
  0.1640414078731069  0.9836323229356623  0.3958951859815443
  0.8546166112044560  0.8891827310328111  0.5874532721955461
  0.5301089097292007  0.2500494531573239  0.4549697690365733
  0.1556323990945003  0.6799006873533884  0.5181536238293987
```

POSCAR file of ZnPSe

```
1.0000000000000000
  6.2164874911589800   -0.0015936773512750    0.0000000000000000
 -0.0012282862422776    6.2316598690952505    0.0000000000000000
  0.0000000000000000    0.0000000000000000   12.7164753336786625
```

```
  Zn   P   Se
  2    2    2
Direct
  0.9545204939889800  0.9806505279081676  0.7100000000000009
  0.4548492879628867  0.4802281807114923  0.7100000000000009
  0.5719710609869821  0.8636245187235971  0.7100000000000009
  0.3379715994684247  0.0975804407689793  0.7100000000000009
  0.8212411593400404  0.3467880590158572  0.7100000000000009
  0.0891144269351898  0.6150474373720911  0.7100000000000009
```

POSCAR file of ZnSSe

```
1.0000000000000000
  5.0977286079590467    0.0038255301973555   -0.0089732282435211
  0.0030653752764559    5.0014394840311143    0.0150684768191558
 -0.0058881066165703   -0.0167270377406591   16.1206315127029356
  Zn   S    Se
   2   2     2
Direct
  0.4459489814800719  0.6729398570405749  0.5007788233250636
  0.9458780464520871  0.1667688379820476  0.4988877064078991
  0.2821482818847088  0.0081199591642545  0.4139291801132927
  0.7830599411223460  0.8319902590616124  0.5856308980466522
  0.5960135144592869  0.3231012485742610  0.4045094871975508
  0.0974892346015039  0.5165568381772587  0.5950509049095416
```

POSCAR file of CdP_2

```
1.0000000000000000
  6.8282318499196926   -0.2100990303539791    0.1006709164078191
  3.0269167547330911    5.6311607518292472   -0.4288666505971974
  0.1646148896751830   -0.9228218137534744   10.5048758616615583
  Cd   P
   3   6
Direct
  0.8421376218447065  0.7713335002592601  0.4072178246394174
  0.1306269338738772  0.0999514529947376  0.4377566248546430
  0.4234229814177439  0.1767725818099919  0.6643502139452764
  0.4944945642881038  0.7214160273948025  0.4125734414816478
  0.7403122825553226  0.1943187607085406  0.5016359942916182
  0.1962601806574540  0.6290508199842293  0.6518781557505733
  0.2106904175130708  0.4591099573489998  0.4500638711440956
  0.4688856784687090  0.7350336509082993  0.6251337080067145
  0.5417295065376351  0.3560551406615886  0.3493852069262928
```

POSCAR file of CdPS

```
1.0000000000000000
  6.4105451151103008   -0.0454654640721711    0.0000000000000000
 -0.0454584953764794    6.4119015623475653    0.0000000000000000
  0.0000000000000000    0.0000000000000000   11.9854837384287300
  Cd   P    S
  2    2    2
Direct
  0.9549430936248697  0.9805887484643065  0.7100000000000009
  0.4550210029718329  0.4806422718827292  0.7100000000000009
  0.5662828632791772  0.8693085490407171  0.7100000000000009
  0.3435055235316824  0.0921029589369411  0.7100000000000009
```

```
  0.8407608425378044  0.3664413646922000  0.7100000000000009
  0.0691547027371371  0.5948352714832836  0.7100000000000009
```

POSCAR file of CdPSe

```
1.0000000000000000
  6.6078598890446454   -0.0438143242241364    0.0000000000000000
 -0.0434417645690472    6.6294225550592847    0.0000000000000000
  0.0000000000000000    0.0000000000000000   11.2459948283500992
  Cd   P    Se
  2    2    2
Direct
  0.9549527727608051  0.9808433934223117  0.7100000000000009
  0.4547893955552027  0.4806212495360001  0.7100000000000009
  0.5639702542781535  0.8715149529434214  0.7100000000000009
  0.3461532894372823  0.0895002041427446  0.7100000000000009
  0.8285819547756574  0.3541130130495489  0.7100000000000009
  0.0812203618754026  0.6073263514061580  0.7100000000000009
```

POSCAR file of α-CdSSe

```
1.0000000000000000
  8.1591664133766475   -0.8156597459168875    0.0711701448945029
  3.2455277057694003    4.6984659661610602    0.3143738596635602
  0.0275353904032876    0.5090457398456393    9.9735603360790570
  Cd   S    Se
  3    3    3
Direct
  0.7382157138246654  0.6671544213178606  0.4977508909672466
  0.2681694390831737  0.9514030188500655  0.5165927898737692
  0.5019075495685499  0.2694819523620708  0.6511653791136567
  0.4671435699923165  0.8131979592392966  0.3050995046642058
  0.7407638870181898  0.1741021952916384  0.4691264986875012
  0.1587936806736607  0.6257393512064695  0.6166970399072369
  0.0884539405536060  0.4775873107696782  0.4357647863259757
  0.5436032735329945  0.7795439391143404  0.7168232634130618
  0.5415091129094805  0.3848317439190225  0.2909748880876322
```

POSCAR file of β-CdSSe

```
1.0000000000000000
  5.4782657931919818    0.0003251313283327   -0.0124362425240665
  0.0002463228093006    5.4744895088923551    0.0302776846877358
 -0.0275871640697543    0.0815984589763995   13.7051634394222255
  Cd   S    Se
   2   2    2
Direct
  0.4459892800669465  0.6693854263174543  0.4998741725577389
  0.9459638748385331  0.1704393772769706  0.4997262226690822
  0.2935751409522709  0.0220383715114281  0.3905358626994513
  0.7959118408036758  0.8178080357300956  0.6090598026556506
  0.5832540040612102  0.3123180620245449  0.3794634176511167
  0.0858438592773751  0.5274877271395155  0.6201275217669675
```

Table S1. Average bond lengths (in Å) in 2D MX_2 slabs.

structure	Zn–P	Zn–S	Zn–Se	Cd–P	Cd–S	Cd–Se	P–P	S–S	Se–Se	P–S	S–Se
α/β-ZnP_2	2.32	-	-	-	-	-	2.38	-	-	-	-
ZnPS	2.28	2.35	-	-	-	-	-	-	-	2.20	-
ZnPSe	2.49	-	2.42	-	-	-	2.31	-	2.35	-	-
ZnSSe	-	2.33	2.46	-	-	-	-	-	-	-	2.25
CdP_2	-	-	-	2.52	-	-	2.26	-	-	-	-
CdPS	-	-	-	2.52	2.58	-	2.05	2.05	-	-	-
CdPSe	-	-	-	2.67	-	2.62	2.05	-	-	-	2.35
α/β-CdSSe	-	-	-	-	2.55	2.67	-	-	-	-	2.25

Table S2. Initial (i) and final (f) average bond lengths (in Å) of 2D MX_2 slabs after AIMD simulation at 900 K.

structure	Zn–P (i/f)	Zn–S (i/f)	Zn–Se (i/f)	Cd–P (i/f)	Cd–S (i/f)	Cd–Se (i/f)
α -ZnP_2	2.42/ 2.50	-	-	-	-	-
β-ZnP_2	2.29/ 2.35	-	-	-	-	-
ZnPS	2.28/ 2.31	2.35/ 2.40	-	-	-	-
ZnSSe	-	2.33/ 2.48	2.46 / 2.51	-	-	-
CdP_2	-	-	-		-	-
α -CdSSe	-	-	-	-	2.55/2.56	2.64/ 2.67
β-CdSSe	-	-	-	-	2.56/2.58	2.68/ 2.84

Table S3. Calculated band gaps of the 2D MP_2 (M=Zn, Cd), MSSe (M=Zn, Cd) and ZnPS slabs at the PBE and HSE06//PBE levels of theory.

structure	PBE (eV)	HSE06//PBE (eV)	direct/indirect
α.ZnP_2	0.41	0.80	indirect
β.ZnP_2	0.70	1.39	direct
ZnPS	1.66	2.62	indirect
ZnSSe	1.62	2.63	indirect
CdP_2	0.57	1.18	direct
α-CdSSe	1.00	1.89	indirect
β-CdSSe	2.04	3.08	indirect

Table S4. Charge density difference (ΔQ) of atoms in 2D MX_2 slabs.

structure	atom	ΔQ	atom	ΔQ	atom	ΔQ
α.ZnP_2	Zn	0.58e	P	-0.42e	-	-
β.ZnP_2	Zn	0.57e	P	-0.53e	-	-
ZnPS	Zn	0.67e	P	-0.22e	S	-0.72e
ZnSSe	Zn	0.75e	S	-0.53e	Se	-0.22e
CdP_2	Cd	0.50e	P	-0.35e	-	-
α-CdSSe	Cd	0.78e	S	-0.49e	Se	-0.71e
β-CdSSe	Cd	0.73e	S	-0.51e	Se	-0.20e

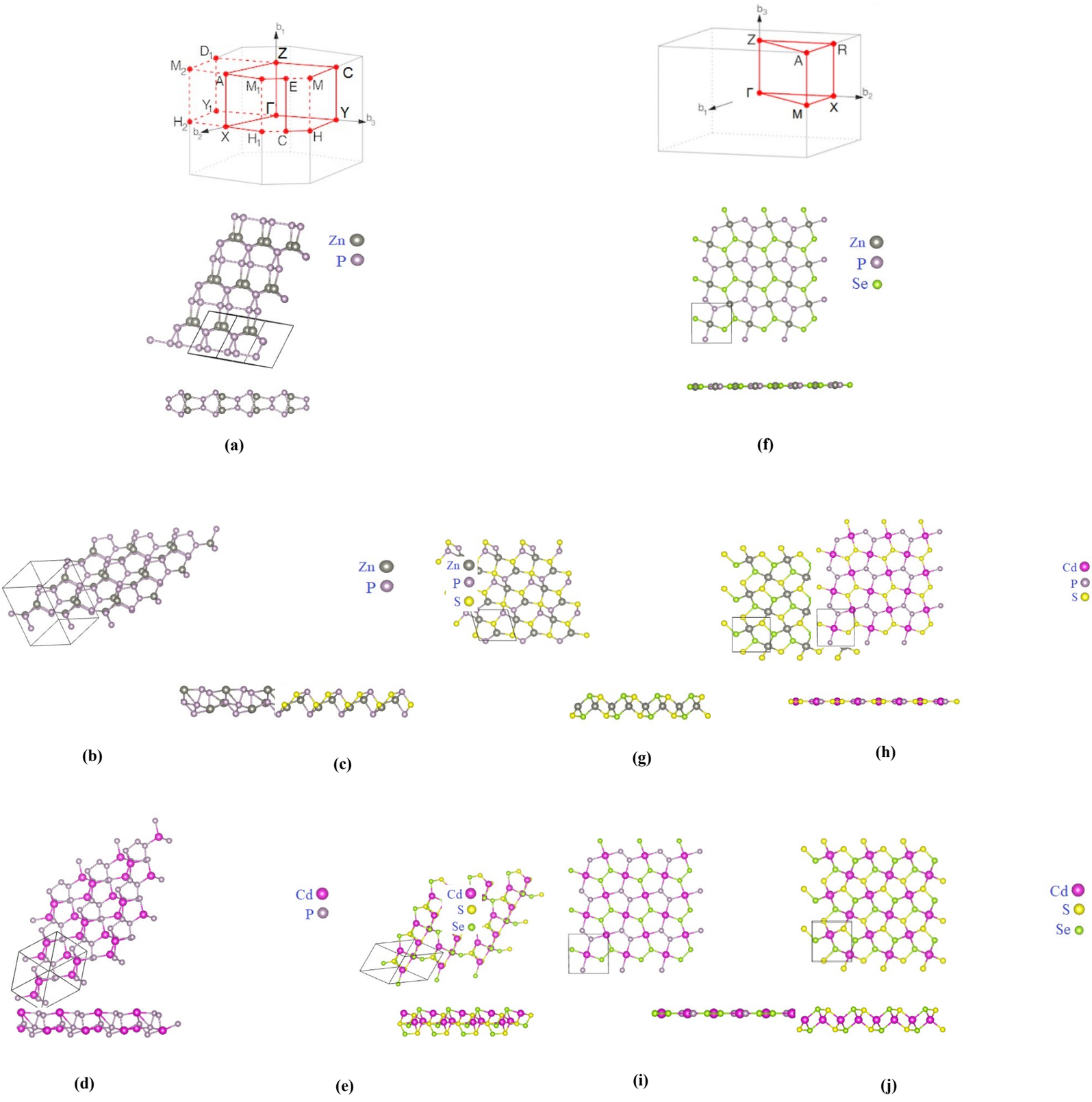

Figure S1. Top-/ side-view of the crystal structures and 2D Brillouin zones including the specific symmetry points, for the following 2D penta-MX_2 compounds: (a) α-ZnP_2 (b) β -ZnP_2 (c) ZnPS (d) CdP_2 (e) α-CdSSe (f) ZnPSe (g) ZnSSe (h) CdPS (i) CdPSe (j) β-CdSSe.

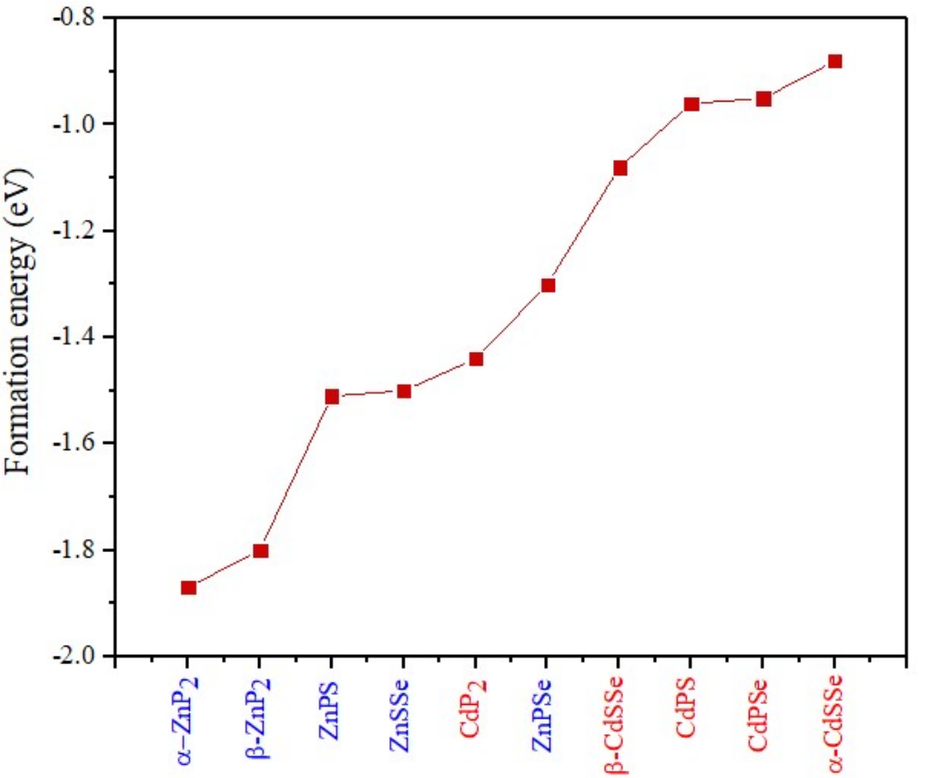

Figure S2. Calculated formation energies of the 2D penta-MX_2 structures (M = Zn, Cd; X= P, S, Se).

ZnP_2

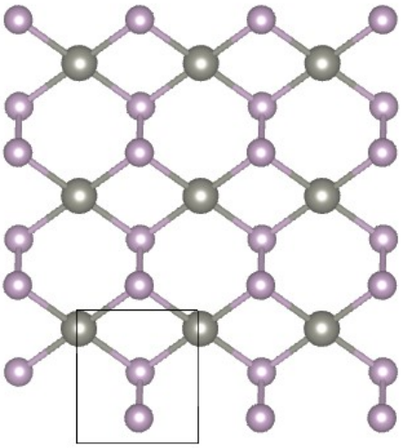

0 eV/atom

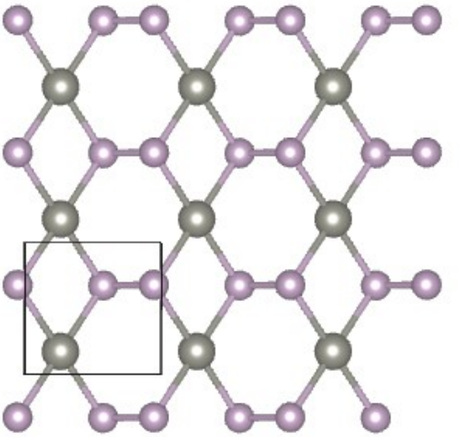

0.01 eV/atom

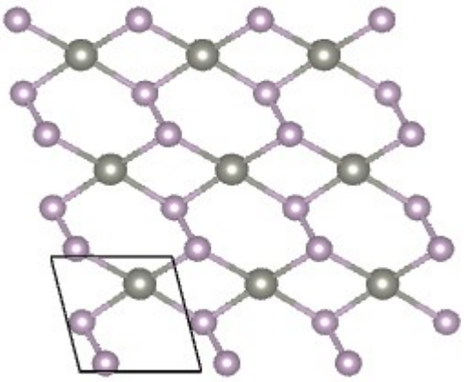

0.15 eV/atom

Figure S3. Relaxed geometry and relative energies are presented for the most stable structure as well as low-lying energy structures of the 2D ZnP_2 compound (Z=1).

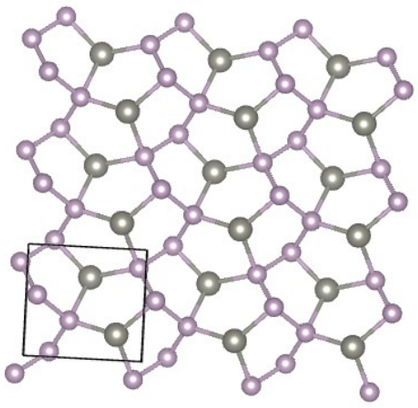

Zn_2P_4

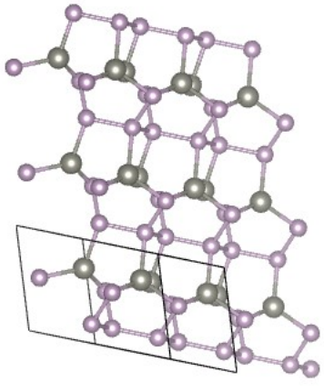

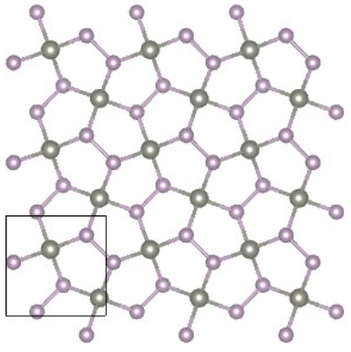

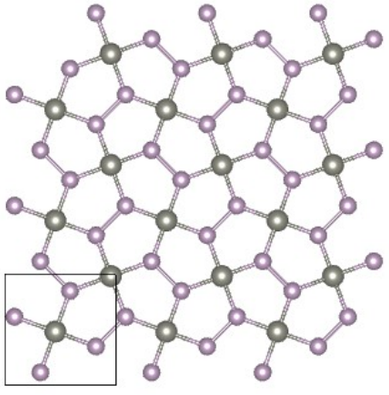

0.20 eV/atom

0.26 eV/atom

0.46 eV/atom

(a)

Figure S4. Relaxed geometry and relative energies of the most stable structure as well as low-lying energy structures for the 2D (a) Zn_2P_4 and (b) Zn_3P_6 structures (Z=2 and 3).

Zn_3P_6

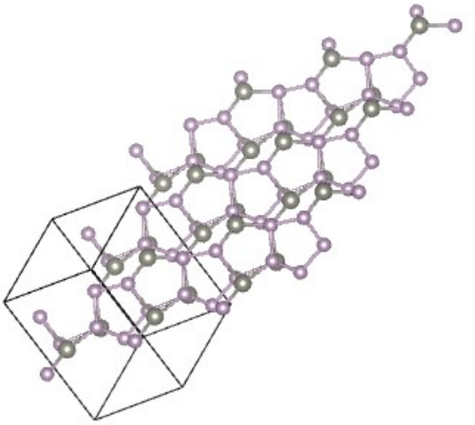

0 eV/atom

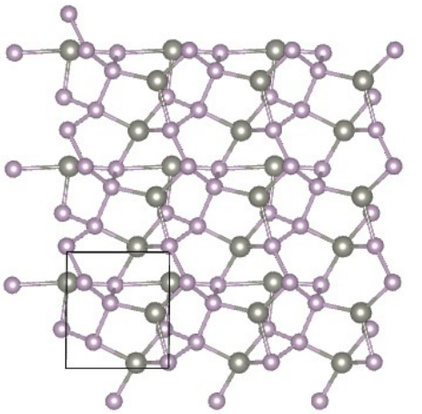

0.05 eV/atom

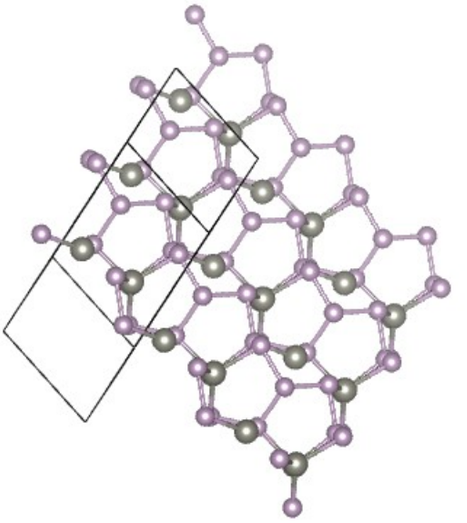

0.09 eV/atom

(b)

Figure S4. Continued.

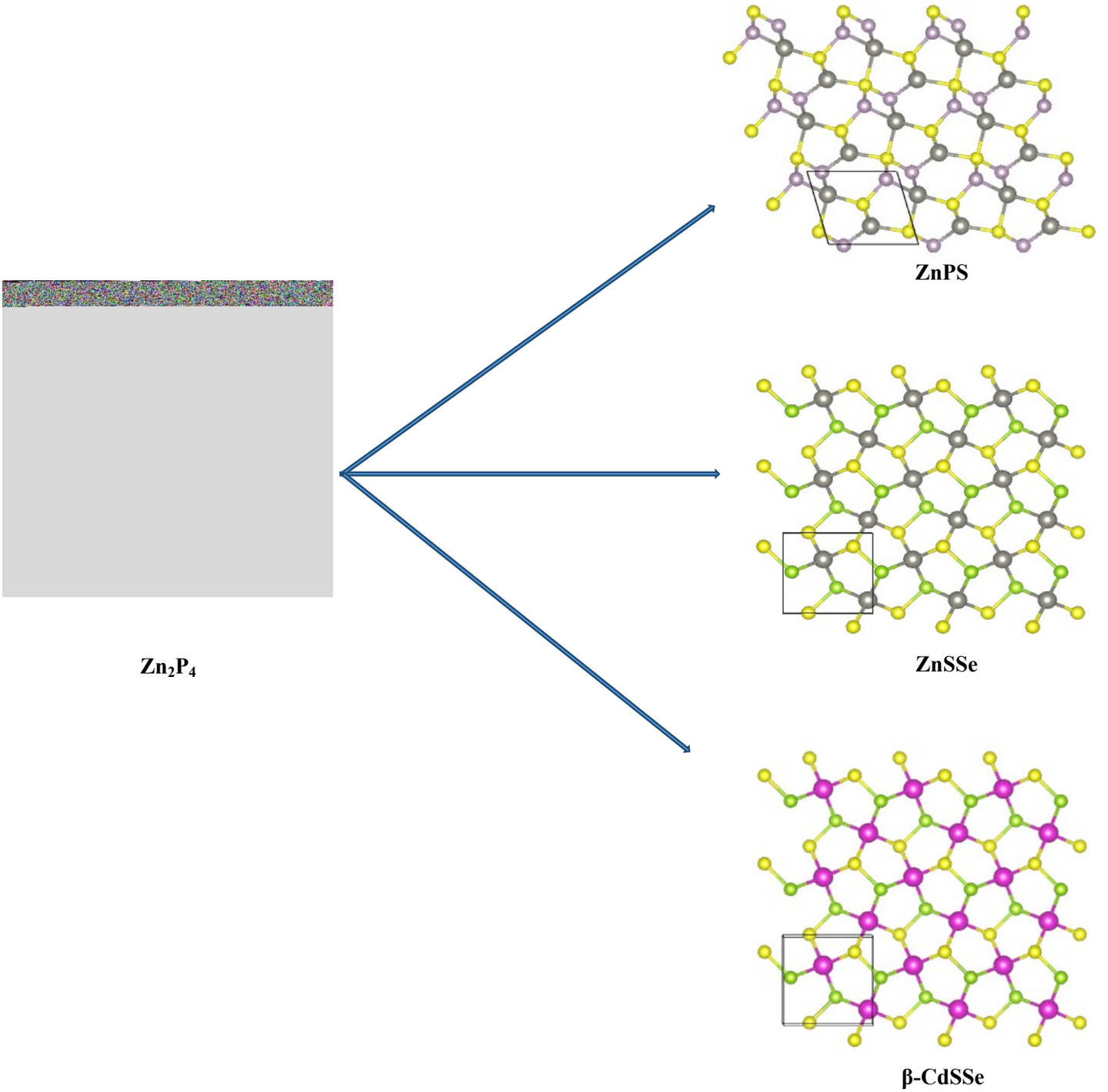

(a)

Figure S5. Design of new pentagonal MX_2 structures; The predicted $(ZnP_2)x$ structures (with x=1,2,3) were used as parents to design new penta-MX_2 structures through the substitution of S/Se and Cd atoms for P and Zn atoms, respectively. The following structures were made: (a) ZnPS, ZnSSe and β-CdSSe, all of which are composed of a Zn_2P_4 structure; (b) CdP_2 and α-CdSSe, composed of a Zn_3P_6 structure; (c) ZnPSe, CdPS and CdPSe, all composed of a Zn_2P_4 structure.

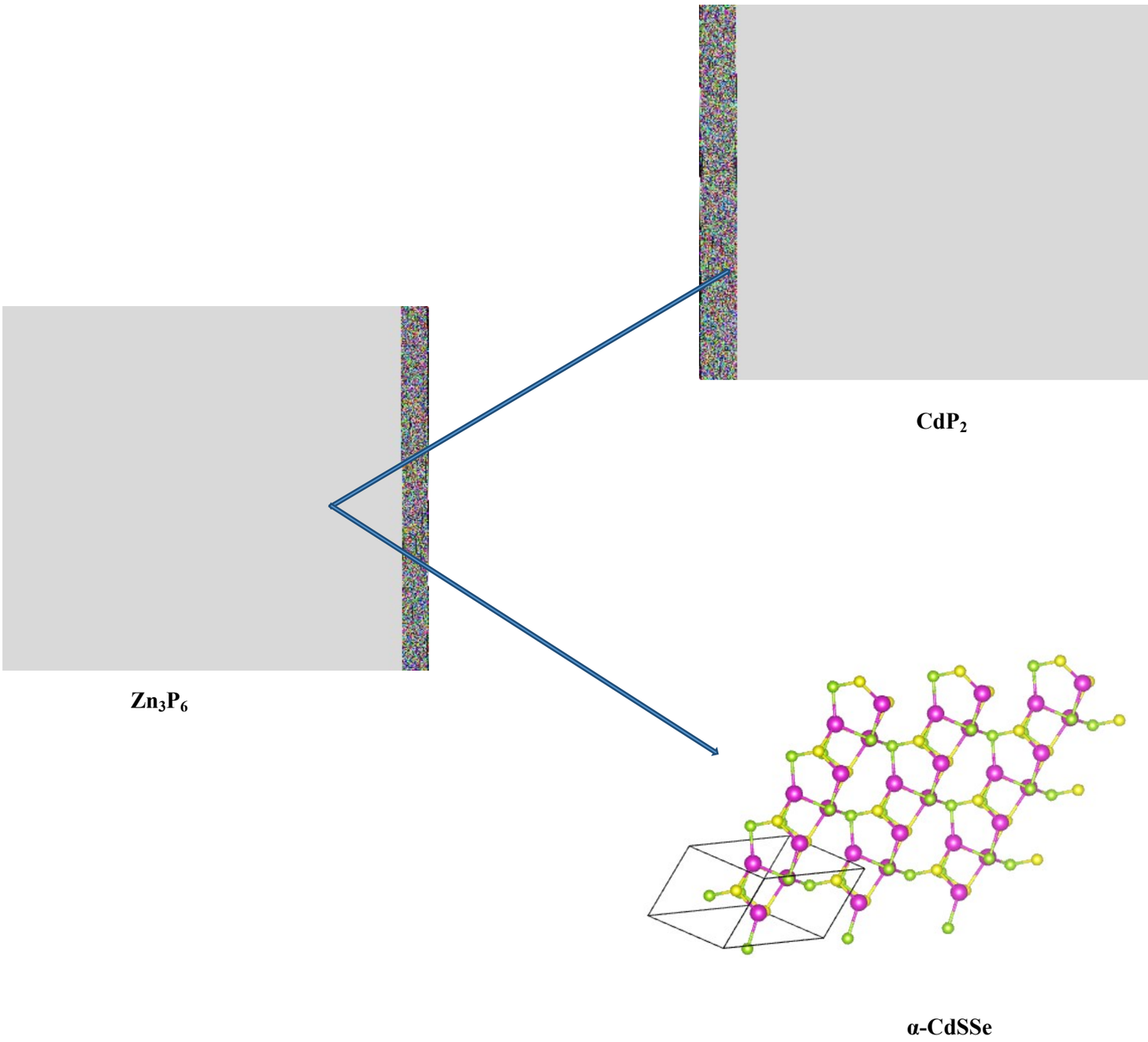

(b)

Figure S5. Continued.

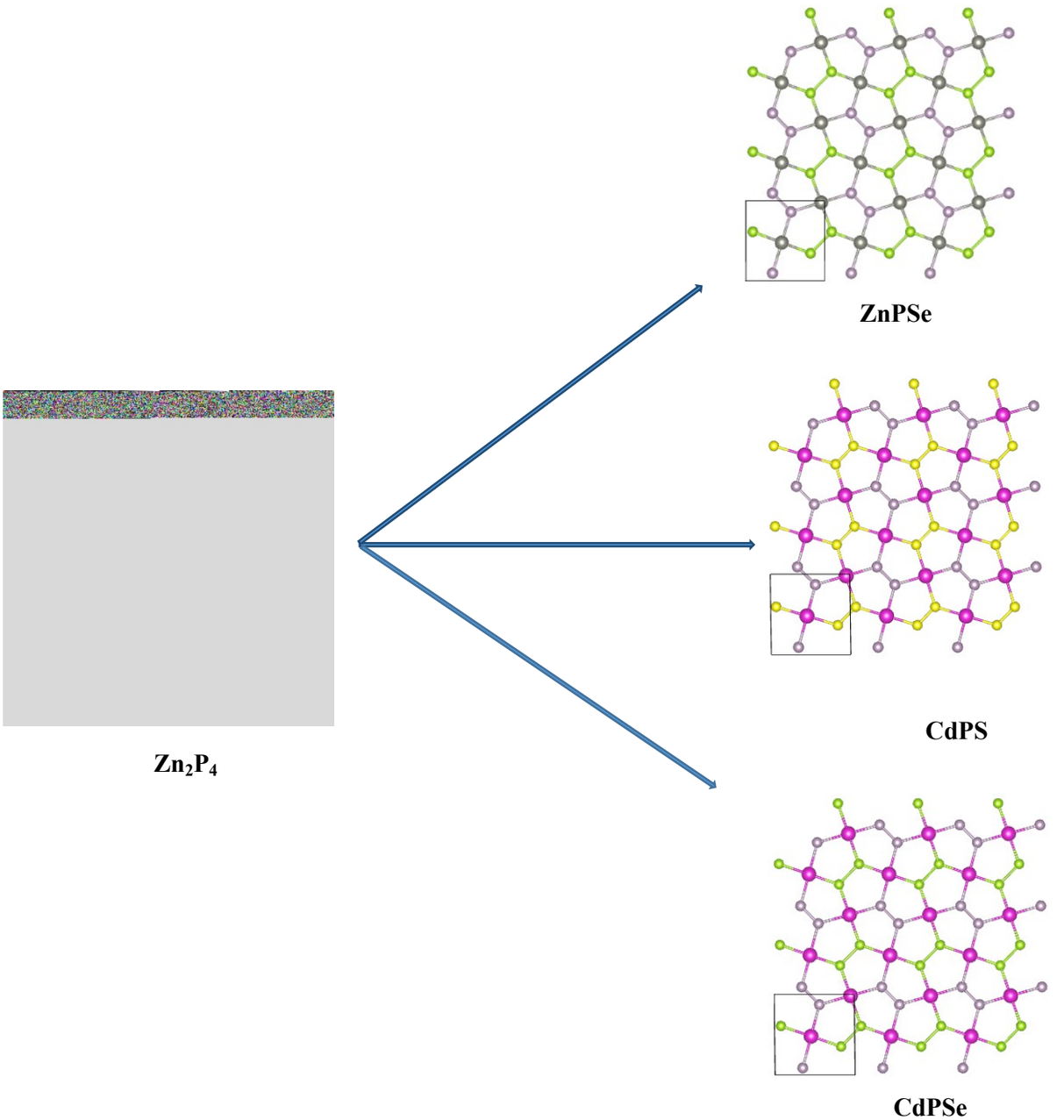

(c)

Figure S5. Continued.

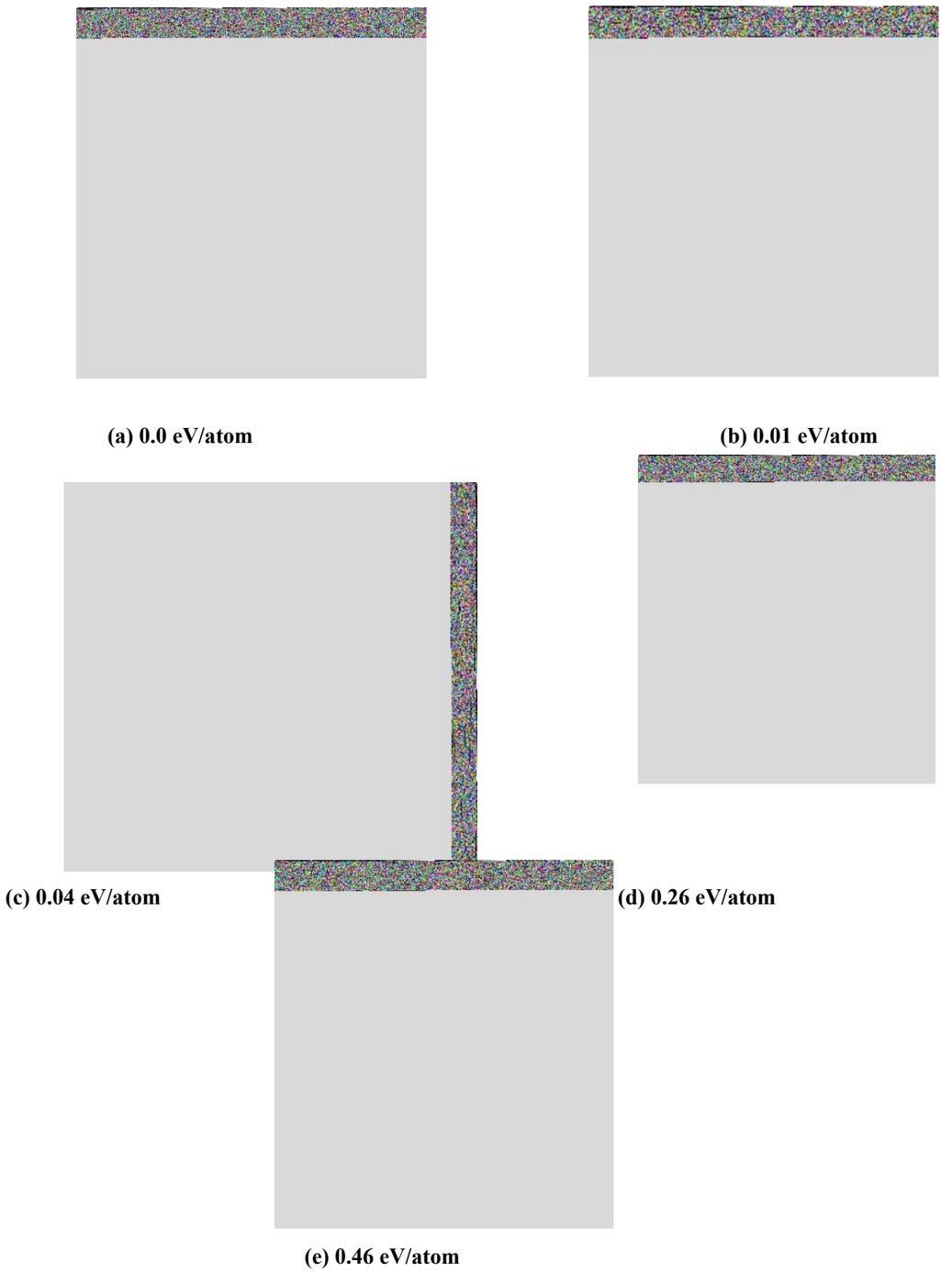

Figure S6. Relaxed geometry and relative energies of the five 2D ZnP2-based prototypes serve as the initial structures of the investigated MX_2. (a) 2D ZnP_2 with infinite non-planar phosphorus chains, (b) 2D α-ZnP_2, (c) 2D β-ZnP_2, (d) 2D ZnP_2 with a Cairo pentagonal tiling, and (e) 2D ZnPS with bent P_2S_2 molecular units.

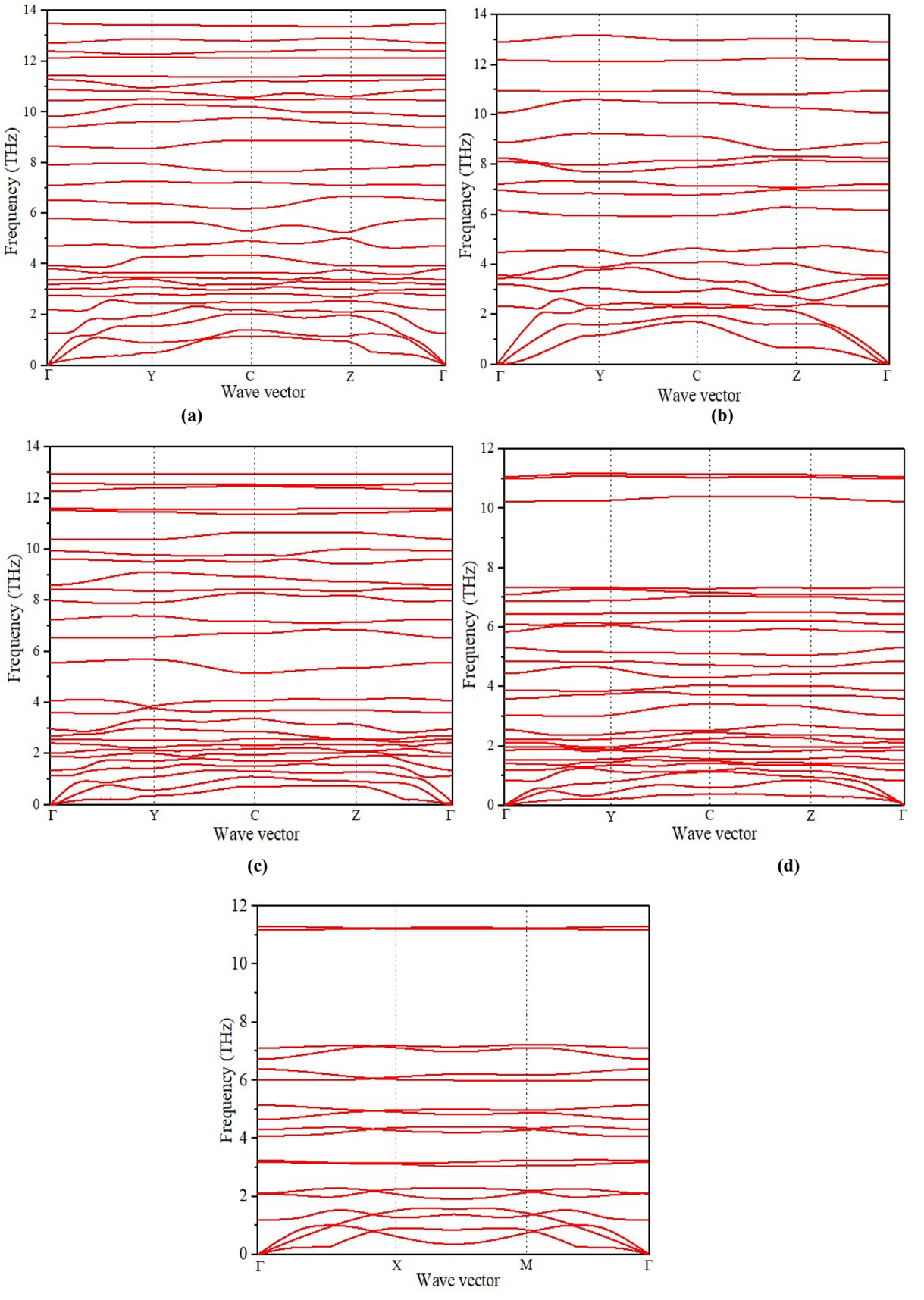

Figure S7. Phonon dispersion curves of the 2D penta- (a) β-ZnP_2 (b) ZnPS (c) CdP_2 (d) α-CdSSe (e) β-CdSSe slabs, along the high symmetric k-point path in the first Brillouin zone.

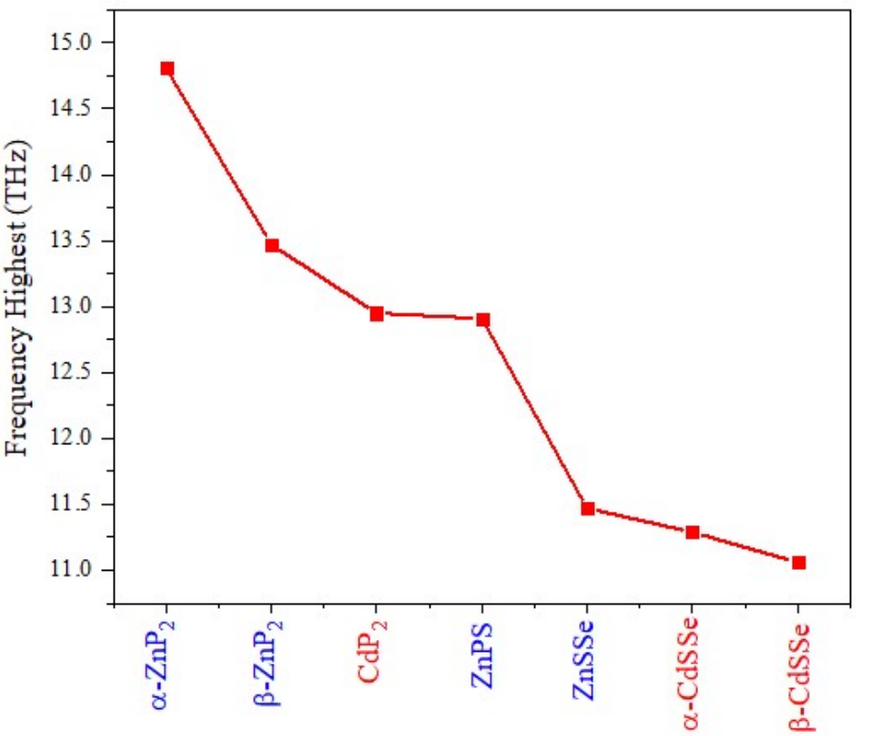

Figure S8. The highest calculated frequency of the 2D penta-MP_2 (M=Zn, Cd), penta-MSSe (M=Zn, Cd) and ZnPS slabs.

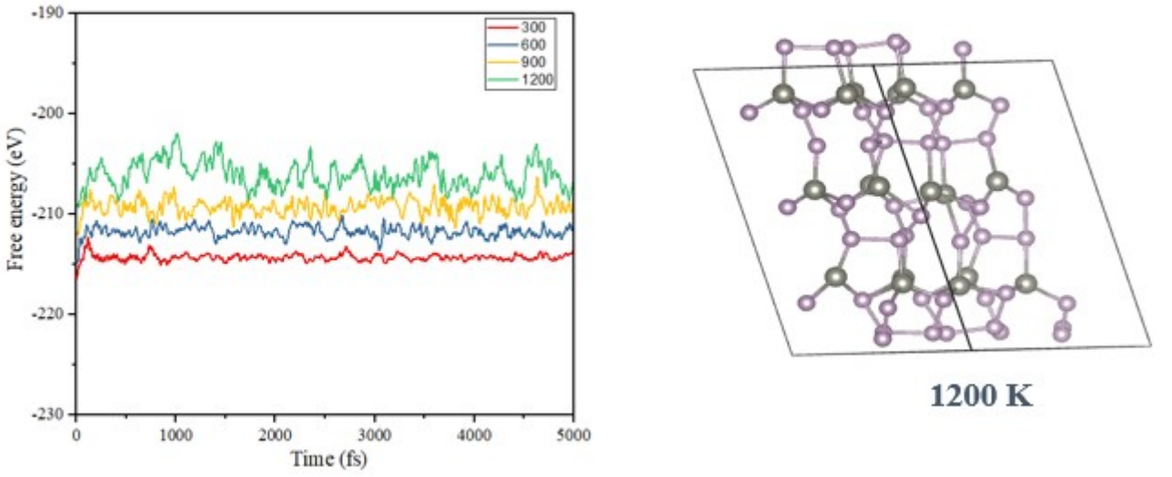

(a)

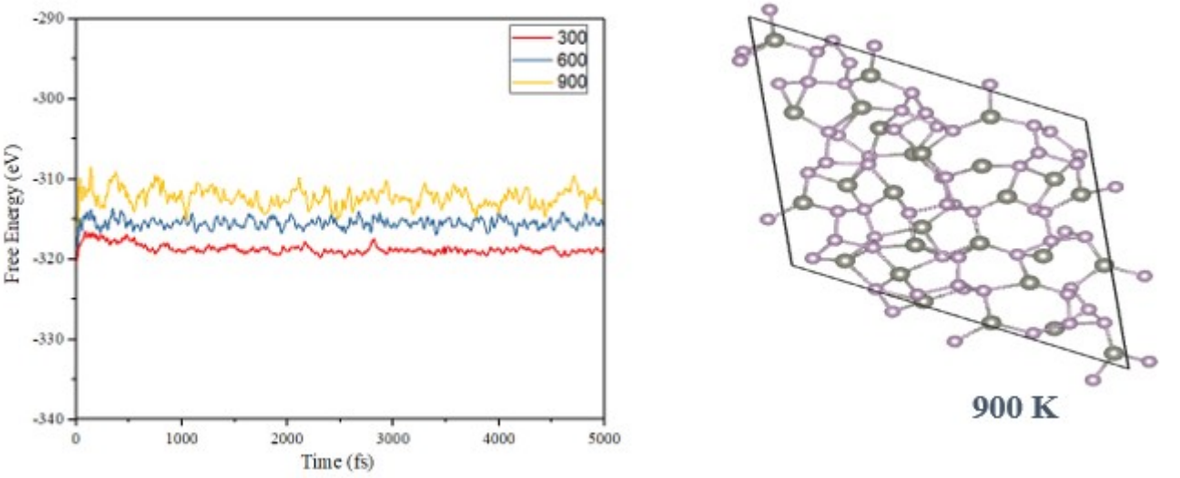

(b)

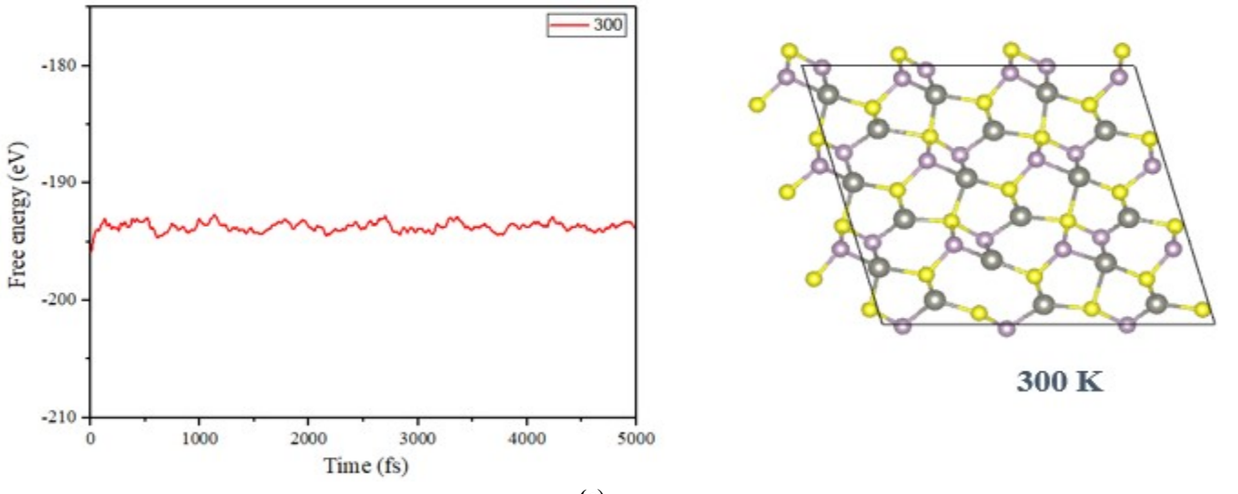

(c)

Figure S9. Energy fluctuations of 2D compounds (a) α-ZnP_2 (b) β-ZnP_2 (c) ZnPS (d) CdP_2 (e) α-CdSSe during the AIMD simulations at different temperatures (in K), and the snapshots of structures at the end of AIMD simulation (5 ps). The grey, pink, yellow, purple, and green balls indicate the Zn, Cd, S, P, and Se atoms, respectively.

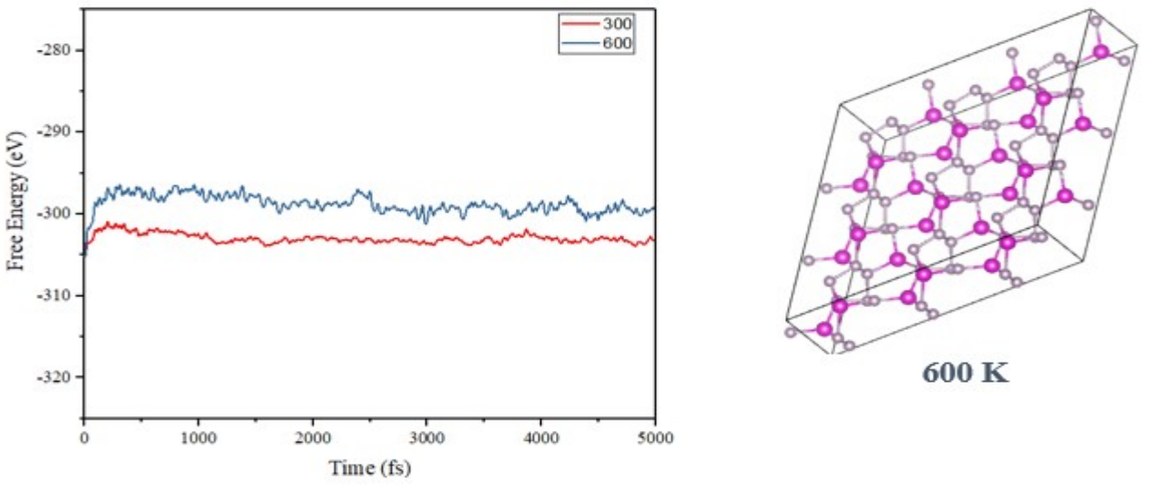

(d)

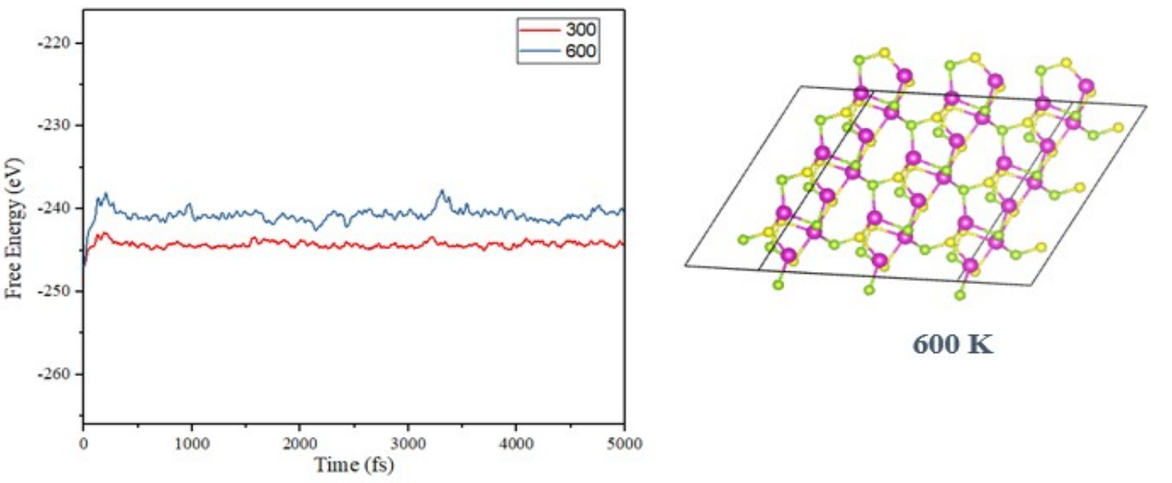

(e)

Figure S9. Continued.

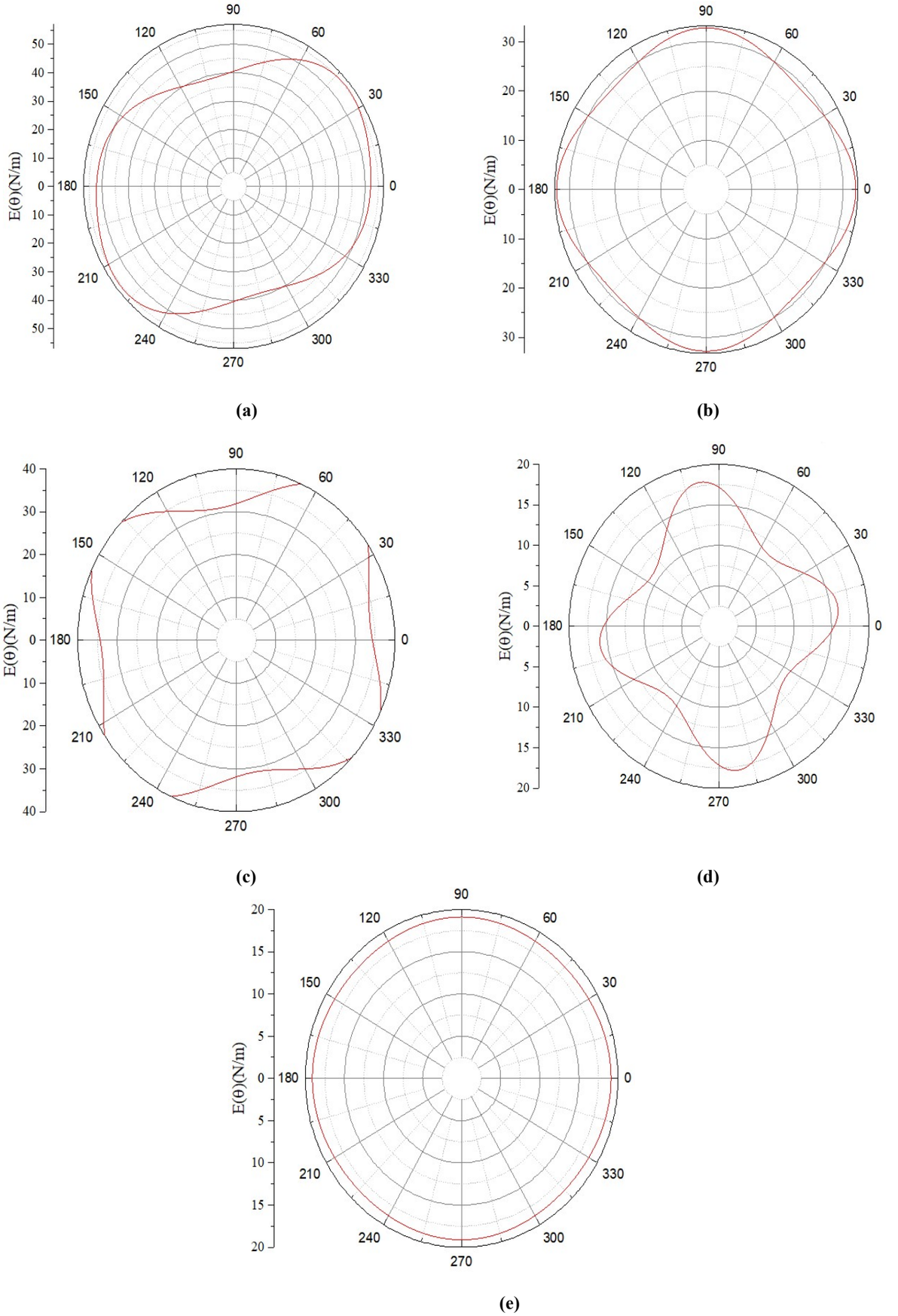

Figure S10. Polar plots of in-plane Young's modulus E(θ) of the 2D (a) β-ZnP_2 (b) ZnSSe (c) CdP_2 (d) α-CdSSe (e) β-CdSSe compounds.

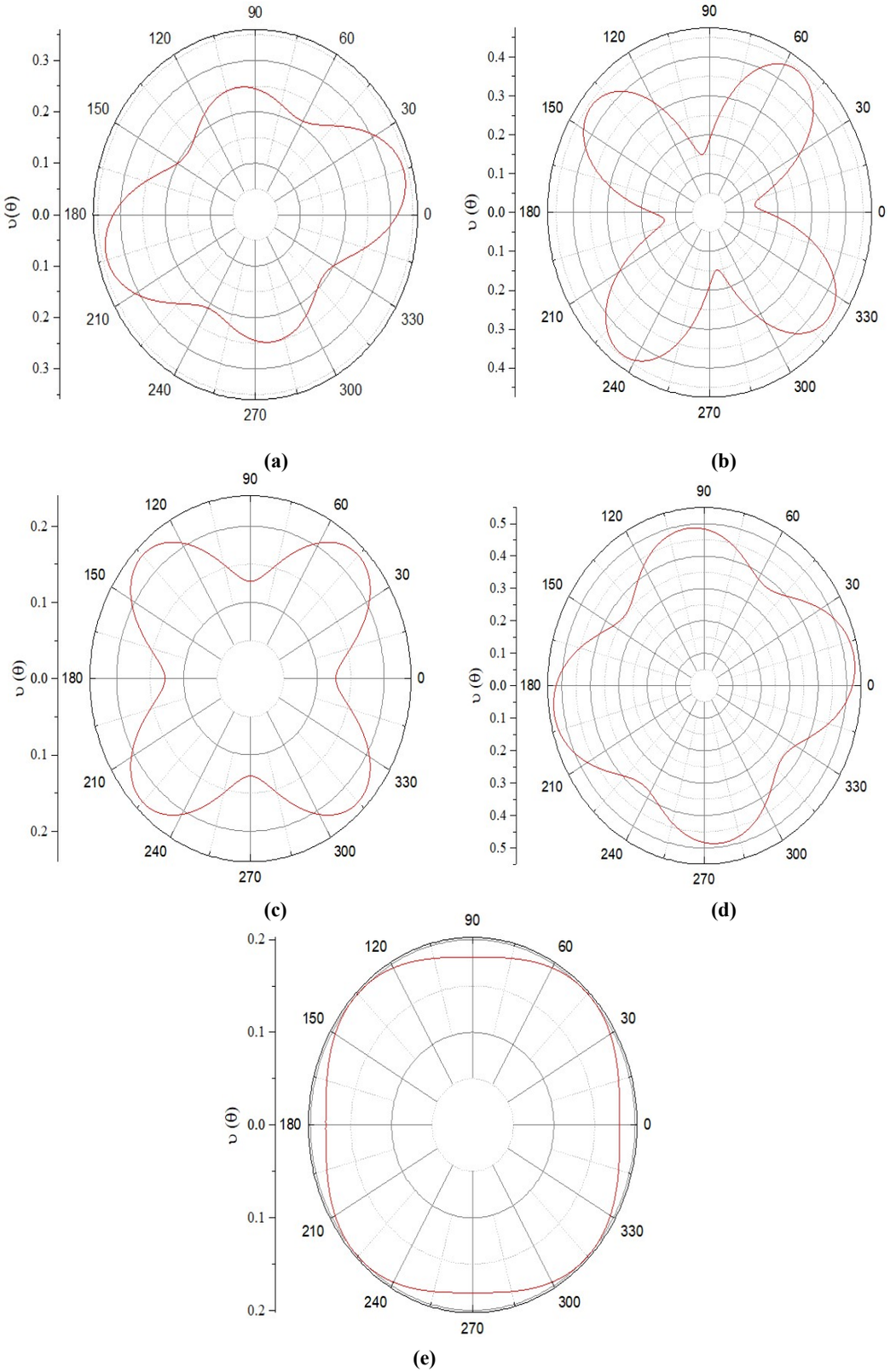

Figure S11. Polar plots of in-plane Poisson's ratio of the 2D (a) β-ZnP_2 (b) α-CdSSe (c) ZnSSe (d) CdP_2 (e) β-CdSSe compounds.

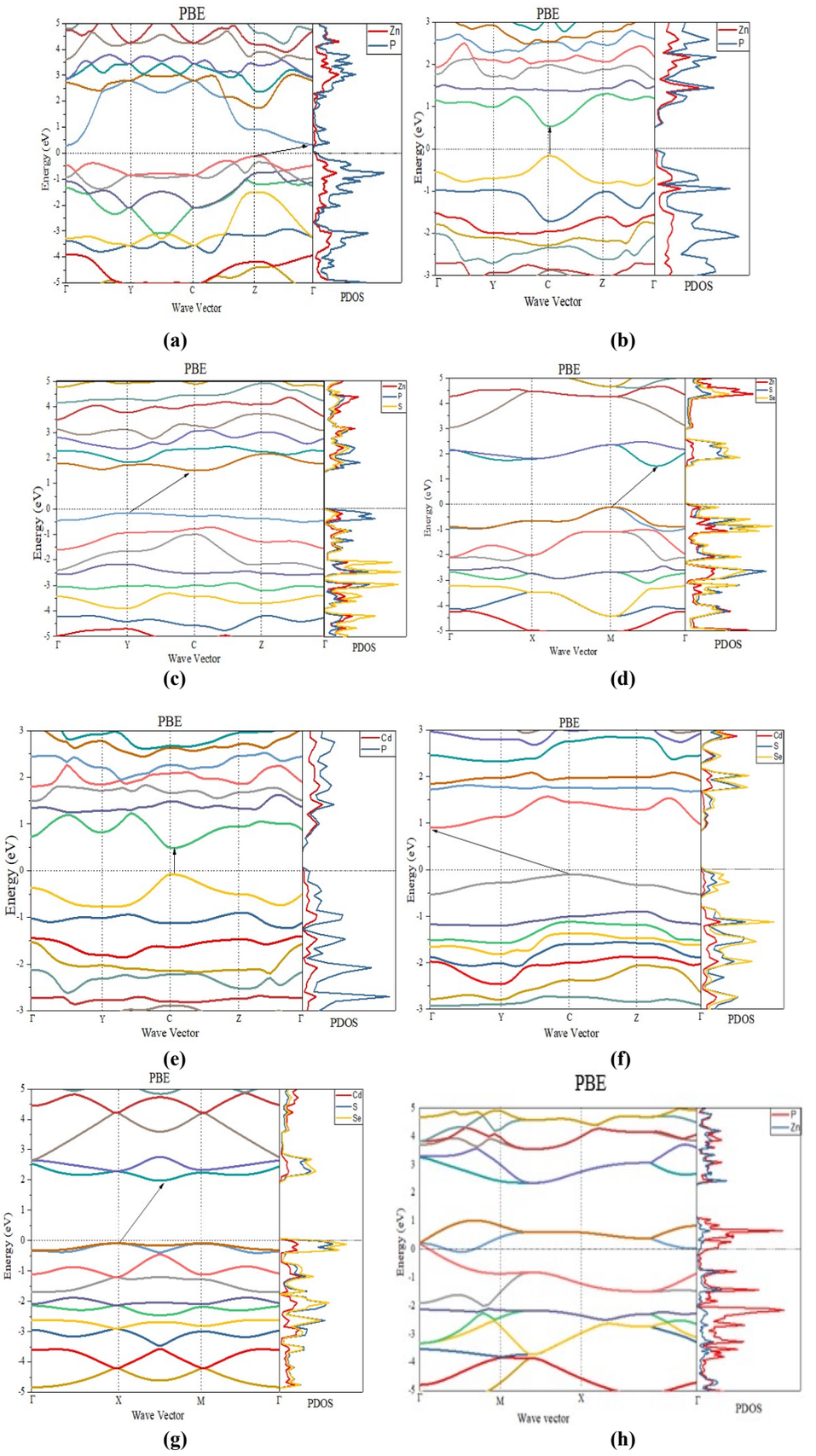

Figure S12. Calculated PBE electronic band structures and projected density of states (PDOS) of (a) α-ZnP_2 (b) β-ZnP_2 (c) ZnPS (d) ZnSSe (e) CdP_2 (f) α-CdSSe (g) β-CdSSe, and (h) ZnP_2 with infinite non-planar phosphorus chains 2D compounds. The Fermi energy is set as zero.

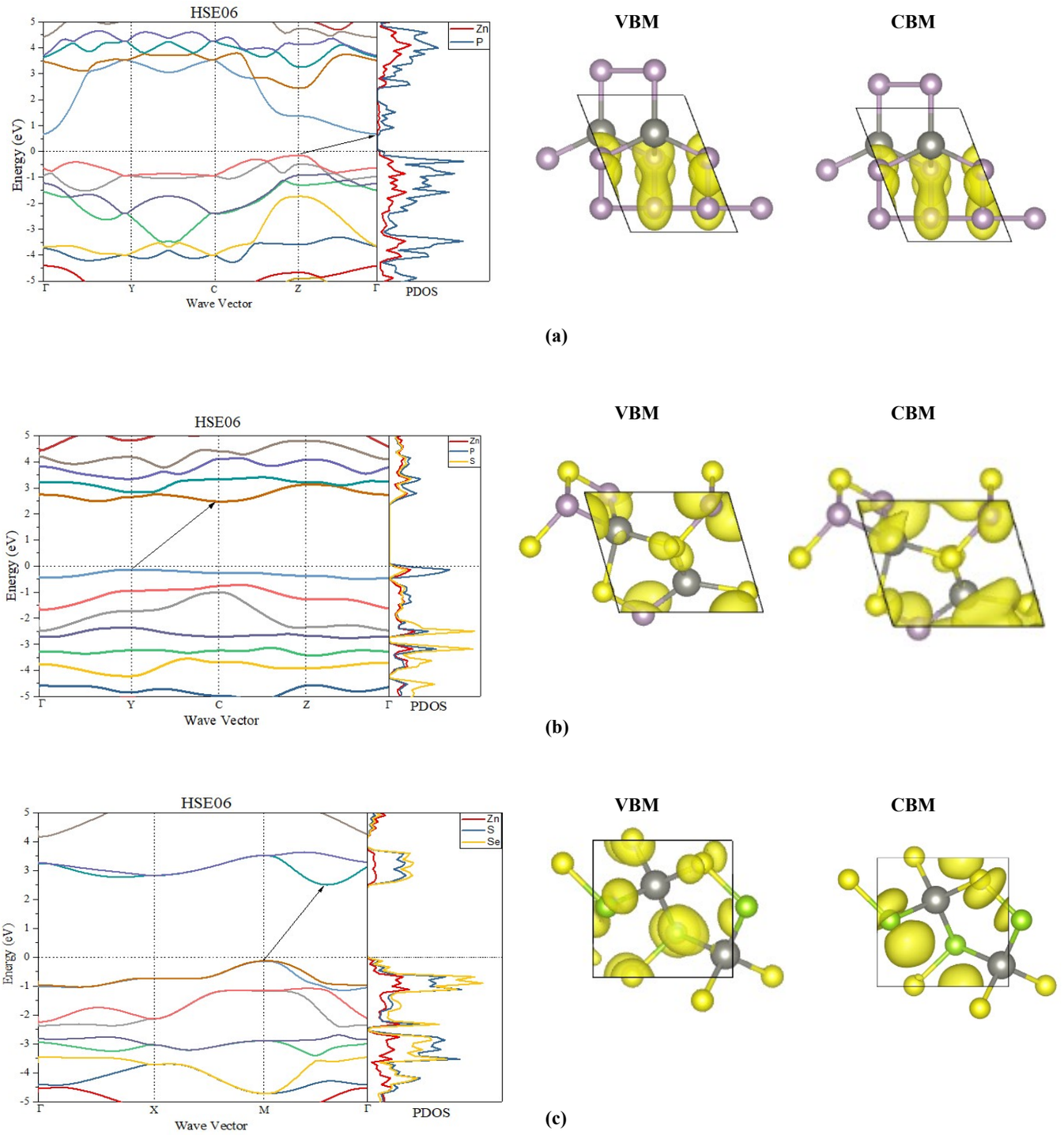

Figure S13. Electronic band structures (HSE06//PBE level of theory), the corresponding projected density of states (PDOS), and charge density distributions of VBM/CBM of (a) α-ZnP_2 ,(b) ZnPS, (c) ZnSSe, (d) α-CdSSe, (e) β-CdSSe, (f) β-ZnP_2, and (g) CdP_2 2D phases. The Fermi energy is set as zero.

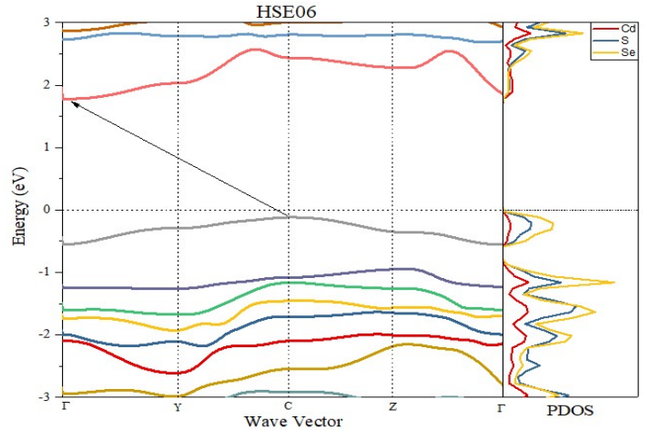

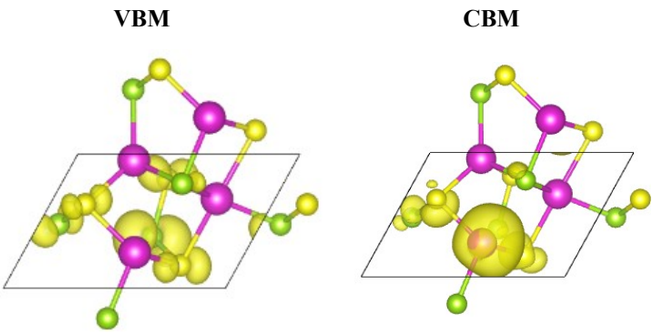

(d)

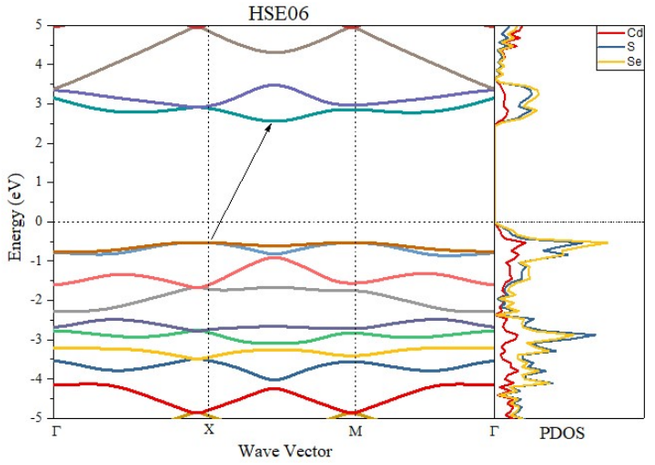

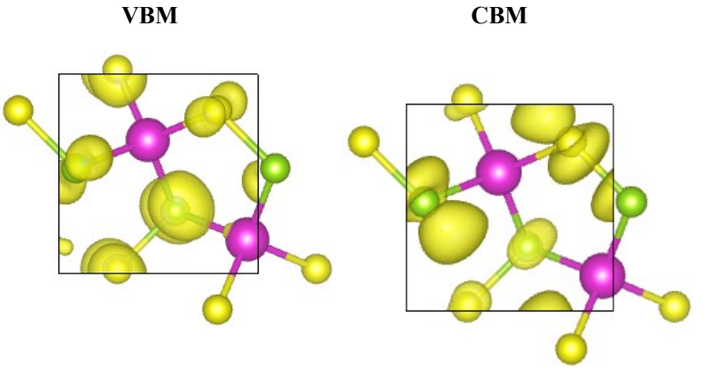

(e)

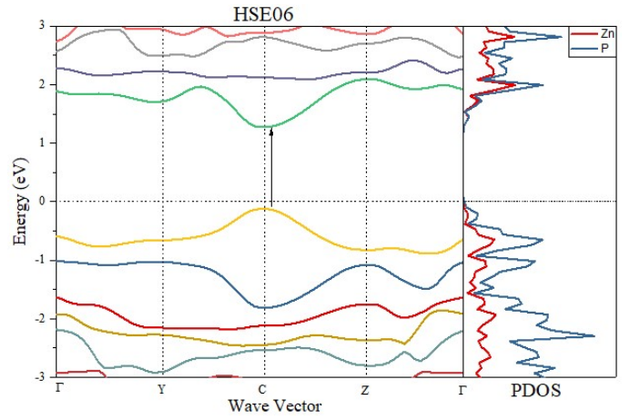

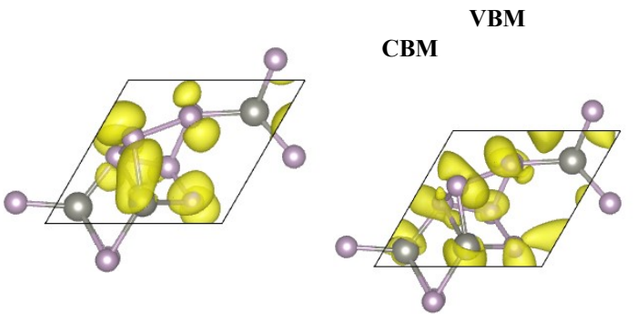

(f)

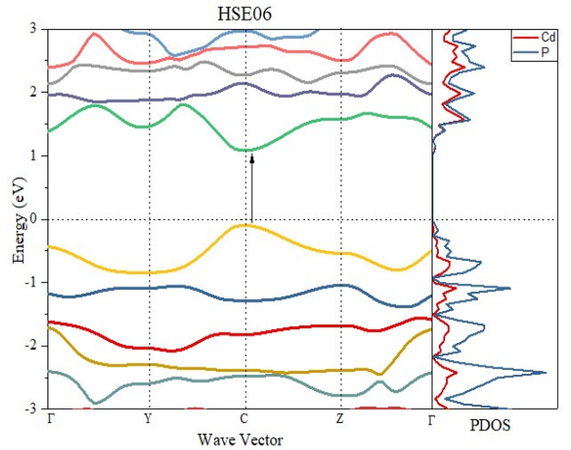

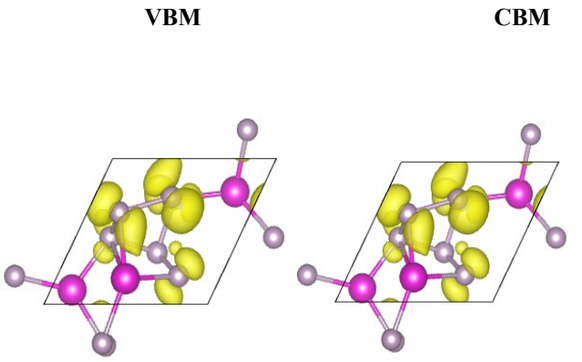

(g)

Figure S13. Continued.

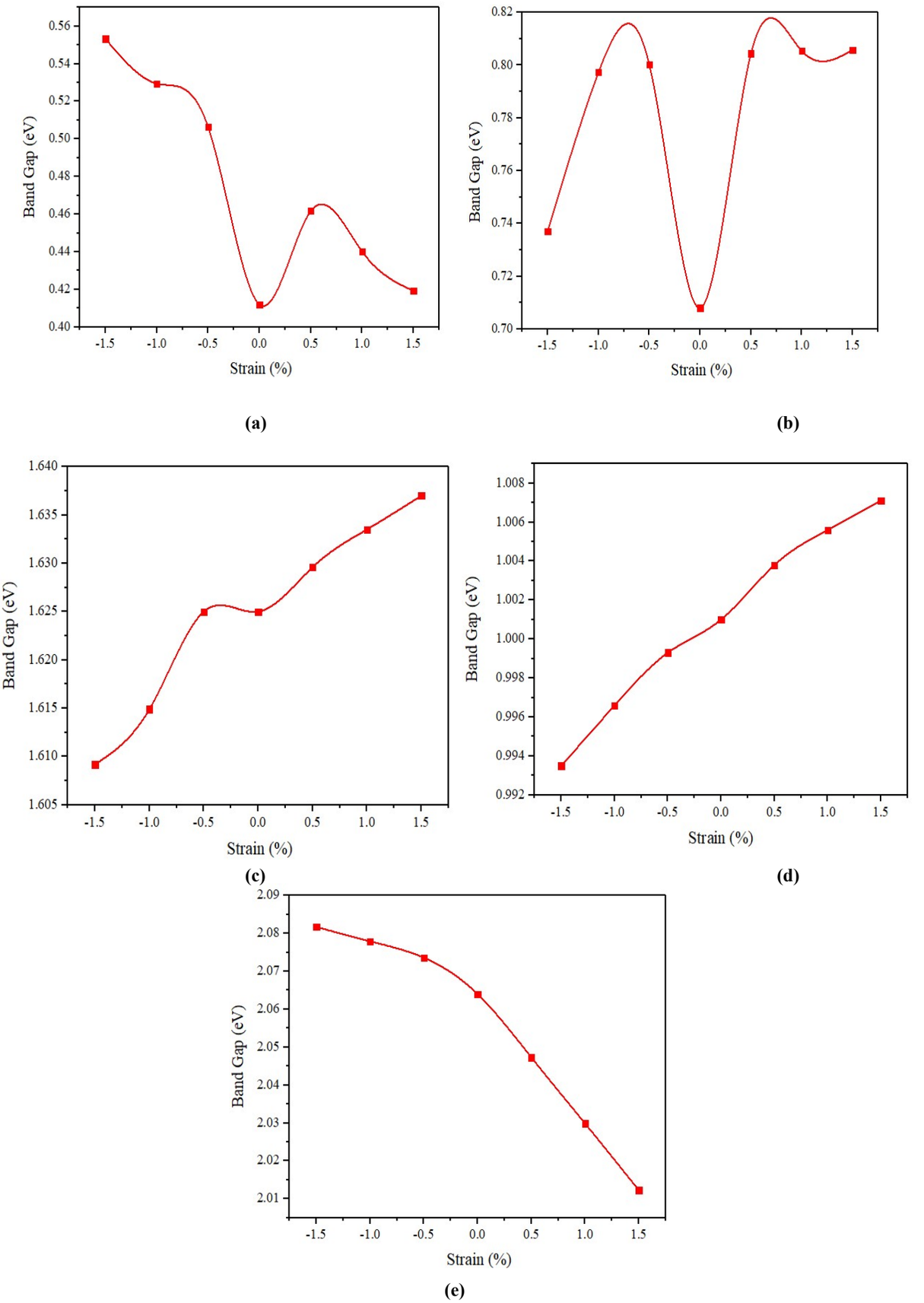

Figure S14. Calculated compressive and tensile strain effects on the PBE band gap of 2D (a) α-ZnP_2 (b) β-ZnP_2 (c) ZnSSe (d) α-CdSSe (e) β-CdSSe 2D compounds.

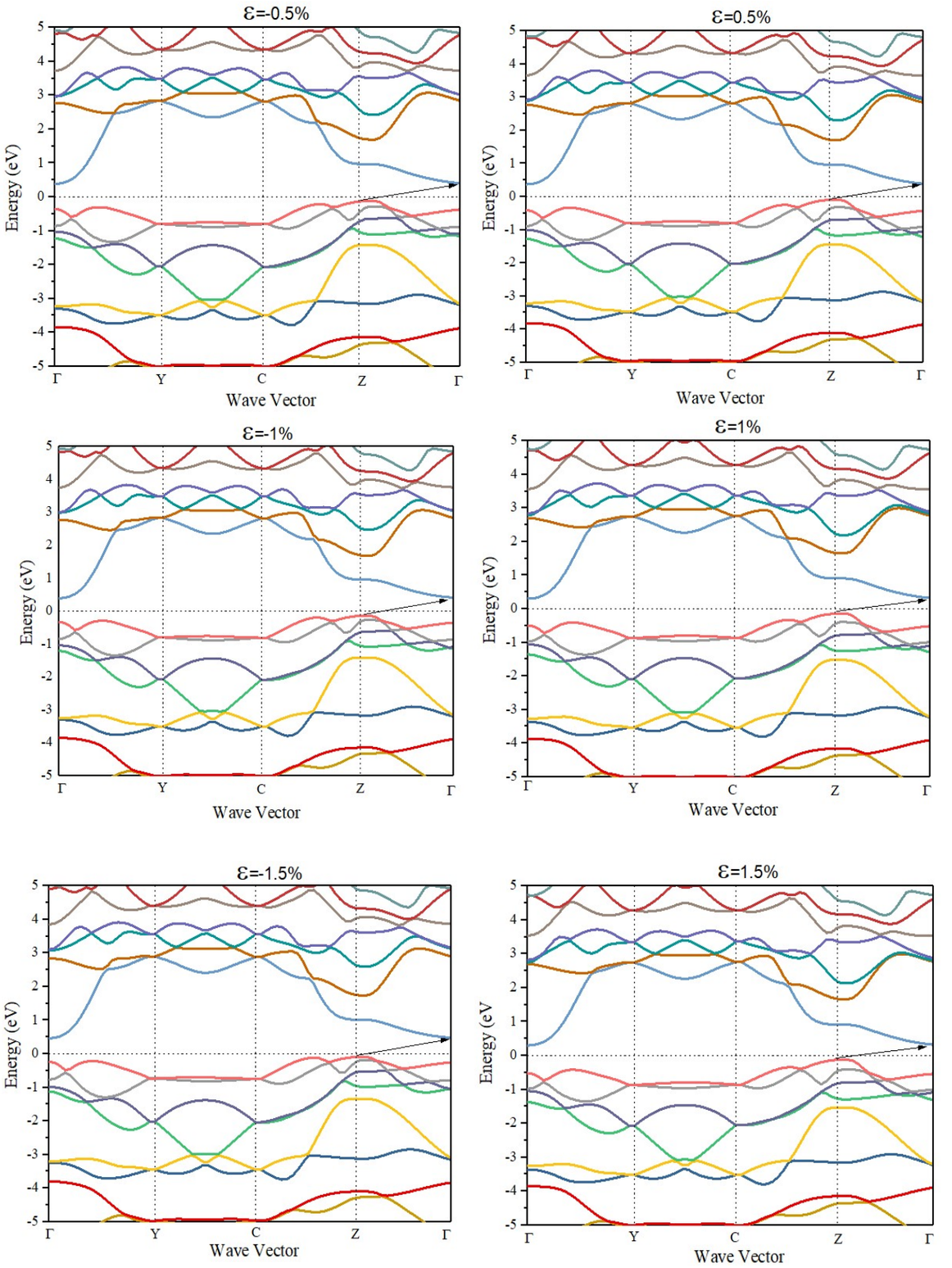

Figure S15. The PBE band structures of α-ZnP_2 under biaxial compressive (left) and tensile (right) strains (ε).

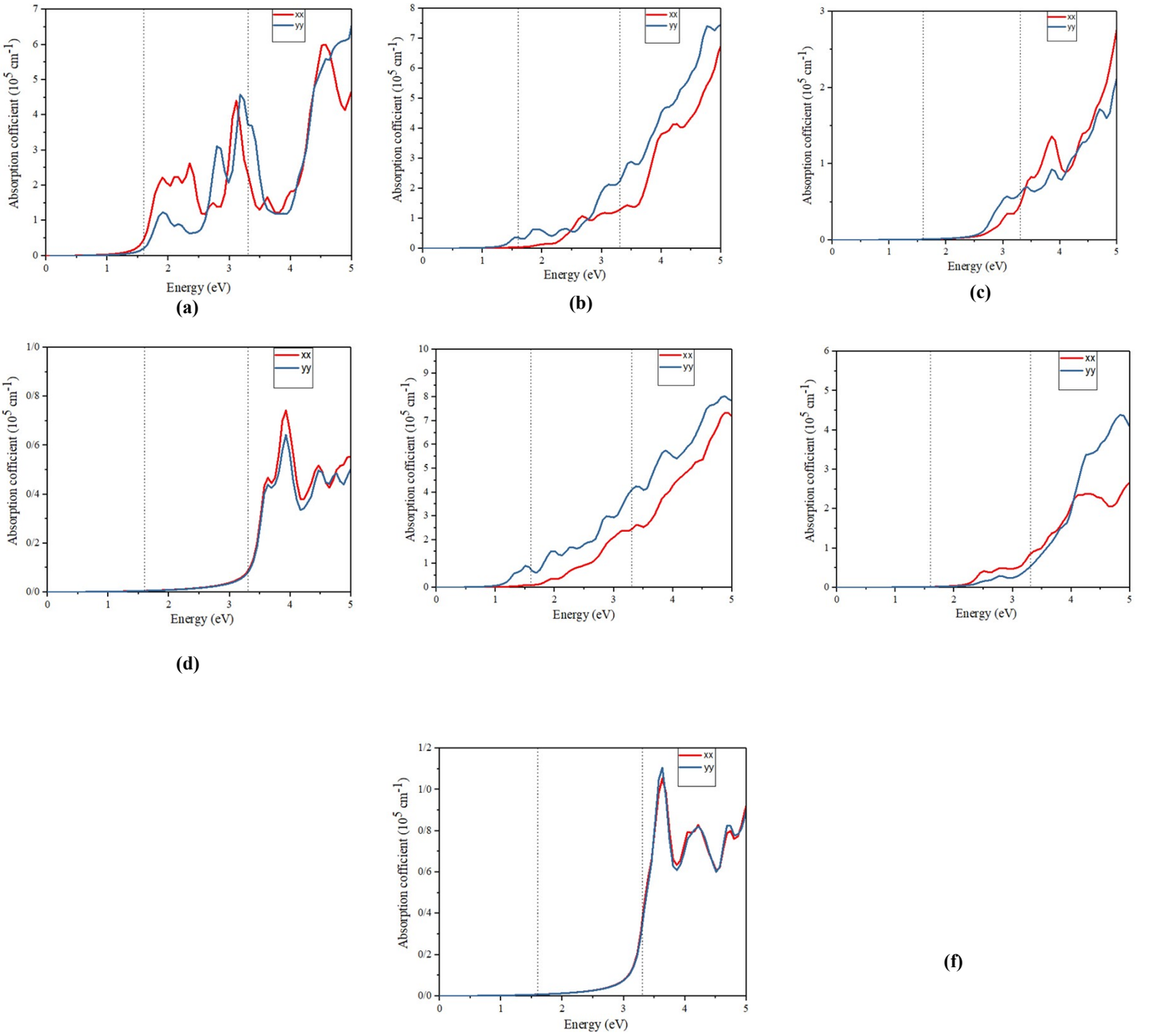

Figure S16. Optical absorption coefficients of (a) α-ZnP_2 (b) β-ZnP_2 (c) ZnPS (d) ZnSSe (e) CdP_2 (f) α-CdSSe (g) β-CdSSe 2D phases along the xx and yy directions from 0 eV to 5 eV. The visible area is marked between the two dotted lines.

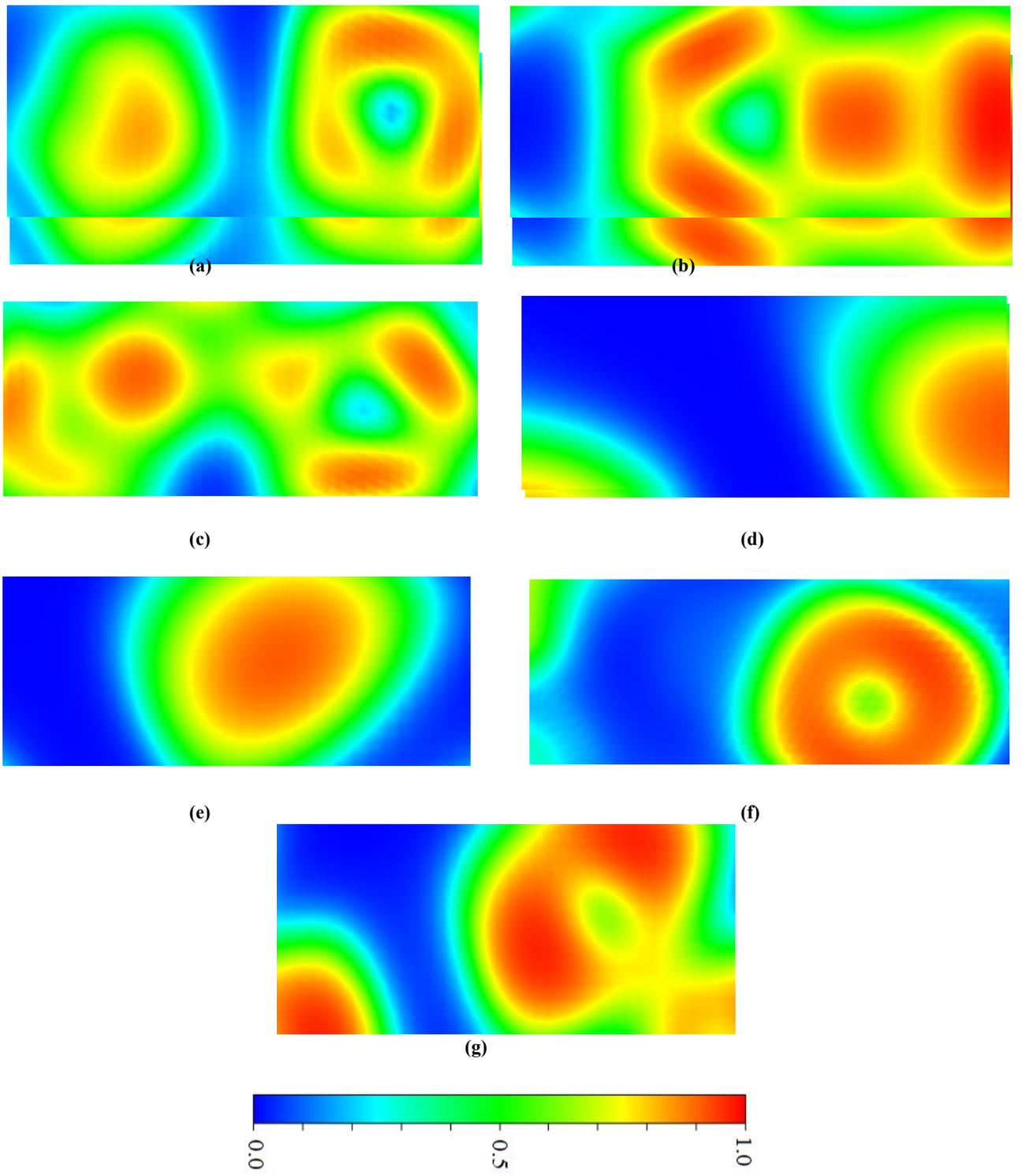

Figure S17. Electron localization function (ELF) of (a) α-ZnP_2, (b) CdP_2, (c) β-ZnP_2 (d) ZnPS (e) ZnSSe (f) α-CdSSe and (g) β-CdSSe 2D phases along the high symmetric k-point path in the first Brillouin zone.

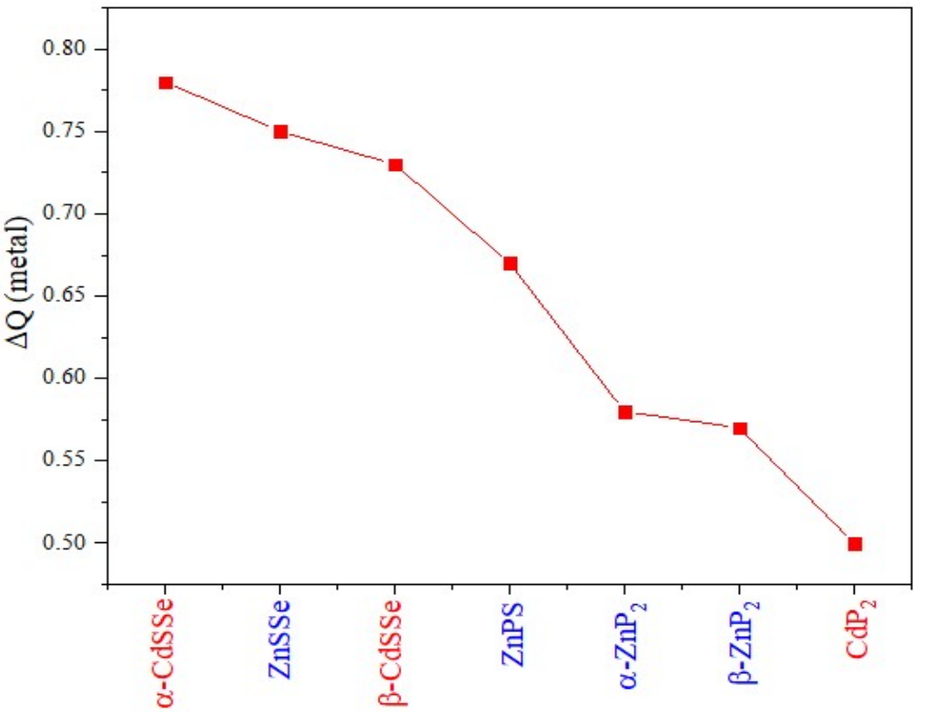

Figure S18. Partial charge density difference (ΔQ) of metal atom in 2D penta-MX_2 structures.